arXiv:0706.3609v2 [cond-mat.supr-con] 24 Oct 2007

Electron Spin Dynamics of the Superconductor CaC_6 probed by ESR

F. Murányi, G. Urbanik, V. Kataev and B. Büchner
Leibniz Institute for Solid State and Materials Research Dresden, 01171 Dresden, PO BOX 270116, Germany
(Dated: February 1, 2008)

Conduction Electron Spin Resonance (CESR) was measured on a thick slab of CaC_6 in the normal and superconducting state. Non-linear microwave absorption measurements in the superconducting state describe CaC_6 as an anisotropic BCS superconductor. CESR data in the normal state characterize CaC_6 as a three-dimensional (3D) metal. The analysis suggests that the scattering of conduction electrons is dominated by impurities and supports the description of superconductivity in the dirty limit. A surprising increase of the CESR intensity below T_c can not be explained by the theoretically predicted change in spin susceptibility. It is interpreted as a vortex enhanced increase of the effective skin depth. The study of the spin dynamics in the superconducting state and the discovery of the vortex enhanced increase of the skin depth poses a challenge to theory to provide a comprehensive description of the observed phenomena.

PACS numbers: 74.70.Ad, 74.25.Nf, 76.30.Pk, 74.25.-q

I. INTRODUCTION

Electron spin dynamics in the superconducting state is a barely studied field. It was predicted some time ago [1][2] that Conduction Electron Spin Resonance (CESR) can be measured in the superconducting state. A decrease of the spin susceptibility, which together with the skin depth determine the CESR intensity, below T_c was predicted by Yosida [3] in the case of no magnetic field. The temperature dependence of the electron relaxation time, T_1, was calculated under the same conditions and predicts an increase of T_1 below T_c [4]. However, to date, only a few experimental works on CESR in superconductors are available. Vier and Schultz [5] observed CESR on thin Nb foils below T_c. They found an increase in T_1 and a significant decrease in the intensity below T_c. CESR has been reported for K_3C_{60} powder by Nemes et al. [6]. They observed a sudden decrease in intensity below T_c and an increase in T_1. CESR on the powder of the two-gapped superconductor, MgB_2, have also been studied [7]. The measured intensity decrease below T_c but the two-gap nature of MgB_2 makes proper analysis difficult. CESR also provides direct access to the conduction band properties of metals and conducting compounds such as intercalated fullerenes [6][8] and intercalated graphite [9].

Recently, a graphite intercalated compound (GIC), CaC_6 has attracted great attention due to the discovery of superconductivity in YbC_6 and CaC_6 [10] with transition temperatures, T_c, of 6.5 K and 11.5 K, respectively. Superconductivity in GICs was first reported in the potassium-graphite donor compound KC_8 with T_c of 0.14 K [11]. Until the discovery of superconductivity in YbC_6 and CaC_6 the highest transition temperature was obtained at $KTl_{1.5}C_5$ with T_c of 2.7 K among all the GICs synthetized at ambient pressure [12]. However, using high pressure synthesis T_c can increase to 5 K in metastable compounds such as NaC_2 and KC_3 [13][14]. Despite its much higher T_c, CaC_6 can also be described as a classical BCS superconductor with an isotropic gap. The zero temperature gap value is ∼1.7 meV [15][16]. The upper critical field, H_{c2}, shows a remarkable anisotropy with the zero temperature value changing between ∼0.4 T and ∼1.9 T, depending on the external magnetic field direction [17].

The scarcity of CESR observations in the superconducting state and the recent discovery of CaC_6 have motivated the present work. Our aims were: i) to obtain insight into the superconducting state of this novel material ii) to study the normal state properties by directly probing the electron spin system by CESR. A striking result of our study is the observation of a surprising increase of the CESR intensity below T_c, which can not be explained by changes in the spin susceptibility. We interpret this observation as an enhancement of the microwave skin depth via vortex dynamics. Our non-linear microwave absorption measuments in the superconducting state support the description of CaC_6 as an anisotropic BCS superconductor. Further, our results on CESR in the normal state characterize CaC_6 as a 3D metal and strongly suggest that the superconductivity can be described in the dirty limit.

II. EXPERIMENT

A) Sample preparation

CaC_6 samples were prepared from Highly Oriented Pyrolytic Graphite (HOPG, Stucture Probe Inc., SPI-2 Grade) and calcium metal (Sigma Aldrich, 99.99% purity). Because the vapour transport method yields only superficially intercalated samples [10] we followed the preparation method of N. Emery *at al.* [18]. Lithium and calcium are strongly water and air sensitive, therefore the lithium-calcium alloy with atomic ratio of 4:1 was prepared in a high purity (O_2 < 1 ppm, H_2O < 1 ppm) argon-filled glove-box. 1 g calcium and 0.7 g lithium (Sigma Aldrich, 99.9% purity) were measured in the stainless steel reactor. The reactor was put on a hot plate in the glove-box. Lithium melts at 180.6 ^{0}C and wets and dissolves calcium pieces. The alloy's melting point is approximately 230 ^{0}C at this atomic ratio. Removal of remaining dirt from the alloy and the mixing of

two components were carried out by a small stainless steel spoon. Due to the high surface tension of the prepared alloy the dirt floats on the surface. HOPG pieces were immersed into the molten alloy with the help of thin tantalum bands. The upper part of the graphite holder fits into the groove formed on the top of reactor holding the graphite in the alloy, preventing the emergence. Another groove was made with a cutting edge inside for sealing. After cooling down the reactor was tightly closed with a copper gasket because lithium vaporizes from the molten alloy and the alloy also captures the remaining oxygen present even in a high purity glove-box. The closed reactor was placed and sealed once more in a stainless steel tube equipped with an other copper gasket. The 10 days long intercalation at 350 ^{0}C was carried out in an industrial furnace to achieve homogeneous temperature distribution. After the intercalation the reactor was opened and heated up on a hot plate in the glove-box. Removed samples were cleaned by sharp knife and sandpaper. The sample's color is gold and the surface possesses a shiny, metallic lustre. The homogeneity of intercalation was checked by scratching the sample from one side to the opposite one. Every slice revealed the same color and brightness, no clue of unintercalated region was found. To check the superconductivity, magnetization measurements were conducted in a SQUID magnetometer.

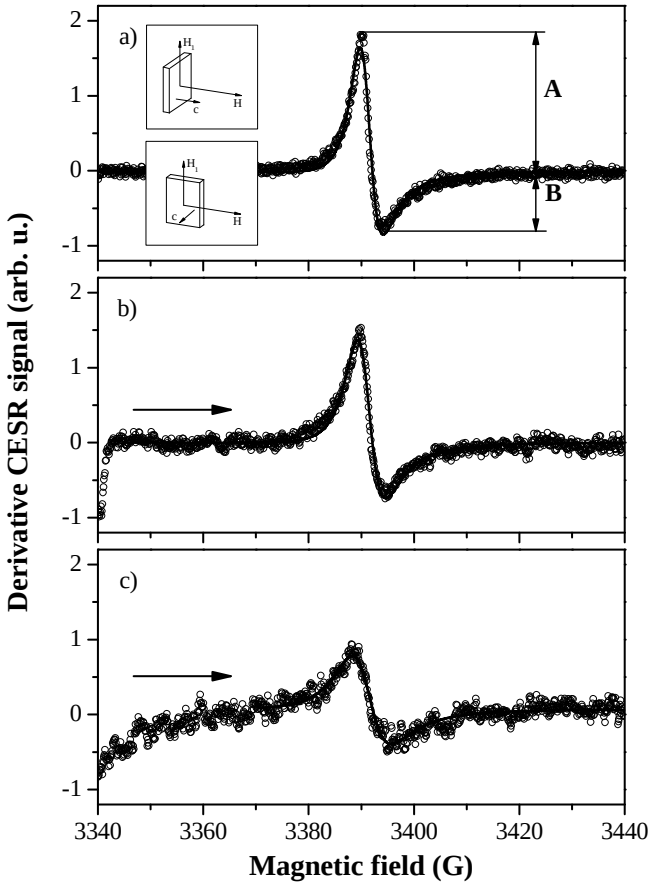


FIG. 1: Selected CESR spectra of CaC_6 recorded at 12.2, 6 and 3.75 K, *a*, *b*, *c*, respectively, H$\|ab$-plane. Open circles represent measured curves, solid lines are Dysonian fits. A/B is the asymmetry parameter, ratio of the maximum, A, and the minimum, B. The arrows indicate the magnetic field sweep direction. Insets show the two magnetic field arrangements: H$\|c$-axis and H$\|ab$-plane. H_1 is the magnetic component of the microwave. For detailed explanation see the text.

B) ESR measurement

ESR measurements were carried out with an X-band (9.5 GHz) spectrometer (Bruker EMX). The sample choosen for ESR measurement with dimensions of 2 x 2.3 x 0.3 mm^3 was glued on to a teflon sample holder with a tiny droplet of vacuum grease (Apiezon N-type) and sealed in a quartz tube under argon atmosphere.

CESR is an efficient tool to characterize GICs because of its sensitivity to the electron spin dynamics and diffusion [9][19]. The analysis of the data was carried out in the framework of the classical Dyson theory [20][21]. Fig. 1. shows selected CESR spectra, field derivative of the absorption, $dP(H)/dH$, recorded at applied magnetic field, H, in the ab-plane. The inset shows the two magnetic field arrangements: H$\|c$-axis and H$\|ab$-plane. The observed lineshape is Dysonian over the whole temperature range studied and is typical of metallic conductors. The resonance field, H_0, the linewidth, w, and the intensity , I, are resulted from Dysonian fits (solid curves). The ratio of the two extrema, A/B, is the so called asymmetry parameter [20], it depends on $\sqrt{T_D/T_2}$, where T_D is the diffusion time, that takes an electron to diffuse through the skin depth, and T_2 is the spin coherence time. For the detailed dependence see Fig. 7. in Ref. [21]. Generally the homogeneous CESR linewidth measures the spin coherence time, $T_2 = 1/\gamma_e w$, where γ_e is the electron gyromagnetic ratio. However, in light metals, T_2, and the spin lifetime, T_1, are equal [22] and therefore the linewidth measures the spin lifetime, T_1, too. Panel *b)* and *c)* of Fig. 1. show the evolution of the CESR line in the superconducting state. The occurance of supercunductivity is indicated by the non-linear start of the magnetic field sweeps and by the enhancement of the noise level due to the so-called vortex noise generated by the magnetic field modulation in the superconducting state below the irreversibility line [23].

III. RESULTS AND DISCUSSION

A) Nonlinear absorption

In the superconducting state the magnetic field dependent nonlinear absorption [24][25] was observed (Fig. 2.). The microwave losses in the superconducting state in the presence of the magnetic field arise due to Lorentz force driven fluxon dynamics. The non-linearity in the microwave absorption disappears when the external magnetic field suppresses the superconductivity. This provides the possibility to estimate the upper critical field, H_{c2}. The results for both magnetic field orientations are

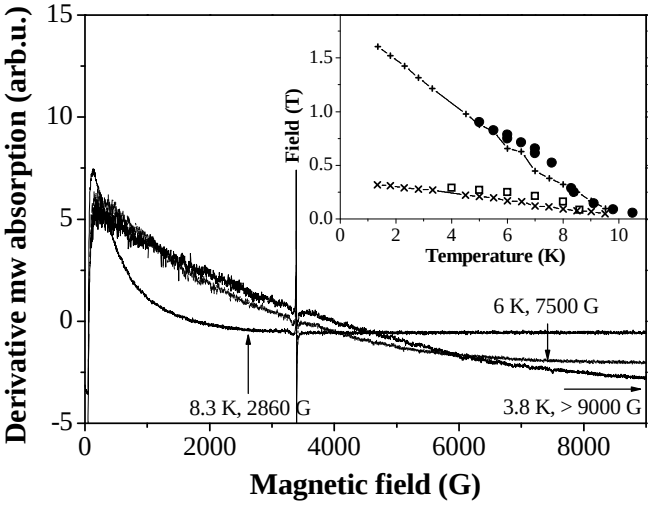


FIG. 2: Non-linear microwave absorption in the superconducting state at 3.8, 6 and 8.3 K, H$\|ab$-plane. Arrows indicate the upper critical field, H_{c2}. Note the sharp signal at 3390 G which is the CESR of CaC_6. Inset shows the measured H_{c2} values. Open squares and full circles denote H$\|c$-axis and H$\|ab$-plane, respectively. $\times$ and $+$ are measured H_{c2} values in Ref.[17].

shown in Fig. 2. inset. The data reveal a linear dependence of $H_{c2}(T)$ with an appreciable anisotropy and thus support the magnetoresistance results of Ref.[17]. Both data sets agree quantitatively well (Fig. 2. inset) and support the description of CaC_6 in terms of an anisotropic BCS superconductor.

B) CESR in the normal state

The CESR results are shown on Fig. 3. The temperature dependence of the g-factor, the linewidth, the asymmetry parameter and the signal intensity were studied in the temperature range 3.8 K $\leq T \leq$ 300 K. In the normal state the g-factor of CaC_6, Fig. 3.a, was measured with an Mn:MgO reference sample with the g-factor of 2.0009 ($\hbar\omega = g\mu_B B_0$, where $\hbar$ is the reduced Planck constant, ω is the angular frequency, μ_B is the Bohr magneton and B_0 is the resonance field). The g-factor of the mother compound, graphite, is highly anisotropic with $g_c = 2.0496$ and $g_{ab} = 2.0026$ [26]. The expectation that intercalation may possibly increase the 2-dimesionality of the mother compound due to the increase of the interlayer distance is not supported by the g-factor values. The measured g-factor, $g_c = g_{ab} = 1.9987(5)$, is orientation and temperature independent below 220 K, which is a characteristic of metals and usual among GICs [9]. The isotropic and temperature independent g-factor supports the assumption that Ca intercalation does not play the role of a simple spacer but creates bonds between the graphene sheets thus increasing the 3D-character of the band structure. A slight anisotropy of the g-factor can be observed above 220 K.

The linewidth in both orientatons is temperature independent and slightly orientation dependent (Fig. 3.b). The calculated spin lifetime for $w \sim 4$ G is $T_1 = T_2 = 1/\gamma_e w = 14.2$ ns. The temperature independent behavior of T_1 means that the spin relaxation is mostly governed by impurities and scattering processes are dominated by disorder. No clear signature of temperature dependence i.e. phonon contribution is present. This justifies the assumption that the superconductivity in CaC_6 can be described in the dirty limit [16] and agrees with the general specifics of the intercalation process, which includes the presence of a certain amount of disorder in the light metal (in this case: Ca) distribution [19]. The linewidth shows a slight anisotropy which decreases with decreasing temperature. This observation and the small anisotropy of the g-factor above 220 K could be interpreted as consequence of a weak anisotropic thermal contraction. It is worth to mention that the Elliott-Yafet relation, $\tau/T_1 \sim \Delta g^2$, [22][27][28] which connects the momentum lifetime, τ, the spin lifetime, T_1, and the deviation from the free electron g-factor, Δg, in light metals does not hold in CaC_6.

The asymmetry parameter, A/B (Fig. 3.c), is related to the ratio of T_2 and the diffusion time, T_D, of an electron through the skin depth [20][21]. In particular, for asymmetries larger than $\sim$3.5, T_D gets comparable and even shorter than T_2. However, in CaC_6 the A/B values lie in the range 1.7-3.3 implying that T_D is much longer than the spin coherence time, T_2. The electron relaxes and looses its spin memory in the skin depth. This conclusion agrees with the presence of disorder in this material (dirty limit). We note that the A/B parameter goes below the theoretical limit in the c-direction. Also in contrast to the theoretical expectation, the A/B ratio slightly decreases with decreasing temperature in spite of the slight increase of the penetration depth. These discrepancies might arise from the layered structure of the studied material, whereas Dyson's theory was developed for an isotropic metal. The layered structure of CaC_6 slightly reflects in the anisotropy of the asymmetry parameter but its values lie in such a range that drawing additional conclusions regarding the diffusion time are not possible.

The temperature dependence of CESR signal intensity, $I(T)$, is determined by the spin susceptibility of conduction electrons and a microwave skin depth, $\delta = \sqrt{\rho/\pi f \mu_0}$ where ρ is the resistivity, f is the microwave frequency (9.5 GHz in our case) and μ_0 is the vacuum magnetic permeability. Fig. 3.d shows the temperature dependence of the normalized intensity, $I(T)/I(300K)$. The intensity was measured with a ruby reference sample (National Bureau of Standards, SRM-2601) placed outside the cryostat and glued on to the cavity wall to keep it at a constant temperature. With the resistivity data of Ref.[17] and [29] the calculation yields a skin depth at 300 K in the c-direction $\delta_c = 5.5\ \mu m$ ($\rho = 115\ \mu\Omega cm$) and in the ab-plane $\delta_{ab} = 3.5\ \mu m$ ($\rho = 46\ \mu\Omega cm$). From 300 K down to T_c the intensity decreases by a factor of 2 and

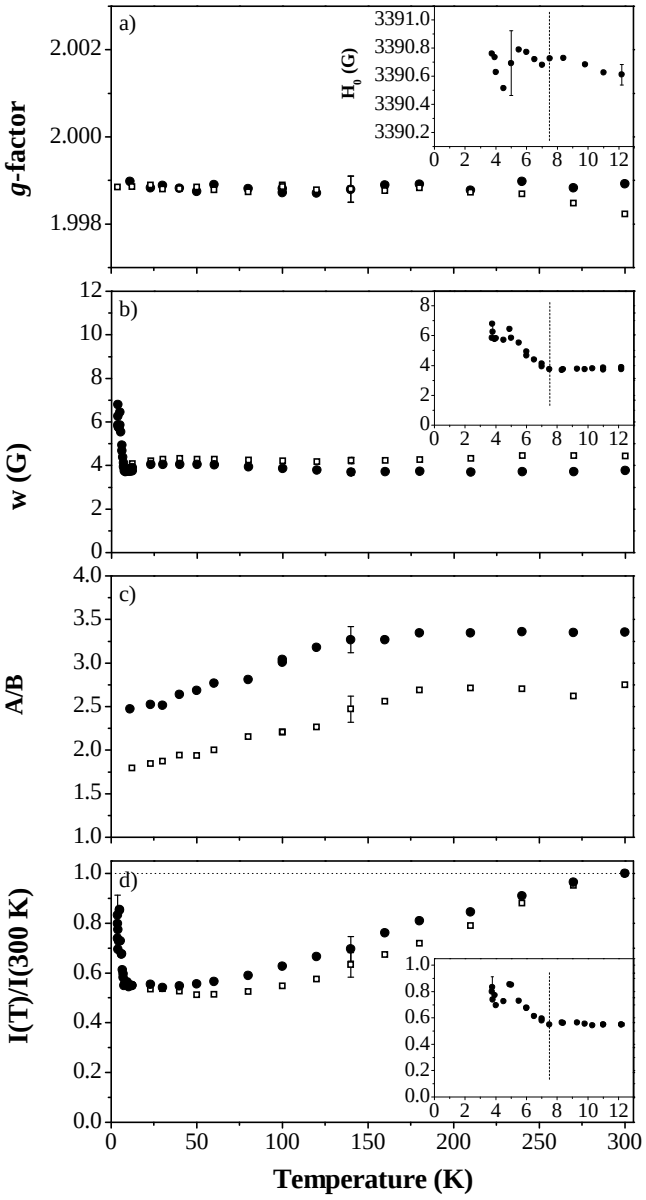


FIG. 3: The temperature dependence of a) g-factor, b) linewidth, w, c) asymmetry parameter, A/B and d) signal intensity, I. Open squares and full circles denote H$\|c$-axis and H$\|ab$-plane, respectively. The insets show the resonance field, the linewidth and the intesity in the superconducting state. Dotted lines indicate the superconducting transition.

there is no significant difference between the two magnetic field orientations. The sample geometry yields that δ_c is relevant for the determination of the volume fraction accessible to microwaves (Fig. 1. inset). Taking into account the temperature dependence of the resistivity in the c-direction [17] it can be concluded that the measured intensity changes in accordance with the change of the skin depth implying that the spin susceptibility is Pauli-like temperature independent. The air sensitive nature of CaC_6 did not allow its proper mixing with an intesity standard for the measurement of the absolute intensity, so we can only give an order-of-magnitude estimation. Taking into account the skin depth the spin susceptibility is $\chi_S \sim 10^{-4}$ emu/mol and assuming negligible electron-electron correlations the density of states at the Fermi-level is ∼3 states/eV. Comparing with theoretical calculation, ∼1.5 states/eV [30], this estimation is reasonable.

C) CESR in the superconducting state

In the superconducting state both w and I show a strong increase below T_c whose origin is obviously related to superconductivity. The critical temperature, T_c, is shifted to 7.5 K at 3390 G (the resonance magnetic field at 9.5 GHz) with H‖ab-plane (Fig. 2. inset). In the other direction, H‖c-axis, these phenomena are not observed since the applied magnetic field suppresses the supercunductivity. The resonance field, H_0 (Fig. 3. a inset), does not change within experimental percision by entering the superconducting state. Existing theories [3][4] do not predict a strong increase of w and I. In the superconducting state of CaC_6 the onset of the irreversibility close to T_c, which is a characteristic of a dirty superconductor, results in an appreciable inhomogeneous broadening of the CESR signal (Fig. 3. b inset). Below the irreversibility temperature the vortex distribution depends on the thermal and magnetic field history [5][6] and causes an inhomogeneous magnetic field inside the sample which makes the determination of T_1 from the linewidth impossible. The magnetic field inhomogeneity arising from the presence of vortices is averaged out because within the lifetime the conduction electrons travel long distances compared to the distance between vortices. The resonance field in the superconducting state in case of MgB_2 is shifted to higher magnetic fields due to diamagnetic shielding currents [7]. The diamagnetic shift is decreasing in increasing magnetic field (see Fig. 2. in Ref. [7]), at $H_0 = 8.1$ T (∼225 GHz) it is only ∼3 G [31]. Comparing the ratio of H_0 and the upper critical field of MgB_2 in the ab-plane, H_0/H_{c2}^{ab} ∼0.5 (H_{c2}^{ab} ∼16 T [32]) with that in the present work H_0/H_{c2}^{ab} ∼0.3 and taking into account that the diamagnetic shift scales with the upper critical field its absence in CaC_6 is reasonable. Surprisingly, the signal intensity (Fig. 3. d inset) starts to increase below T_c in contrast with the theoretical prediction that the spin susceptibility decreases below T_c [3]. A similar behavior has been reported from MgB_2 samples in Ref.[33]. However, the authors related the intensity increase below T_c to paramagnetic centers which show Curie-like spin susceptibility in the normal state. This can not be the explanation in our case because CaC_6 shows temperature independent (Pauli) spin susceptibility in the normal state [34]. A possible explanation is based on the temperature and magnetic field dependence of the skin depth because the CESR intensity on a thick sample is also proportional to the skin depth. An increase of the skin depth as a function of magnetic field has previously been reported on $YBa_2Cu_3O_y$ crystals in

the MHz frequency regime [35]. Qualitatively we can relate the observed increase of the CESR intensity to the increase of the effective skin depth in the superconducting state due to the presence of vortices [36][37]. The applied microwave field interacts with the vortices at the surface and exerts forces on the vortex ends. The evolving deformation of the vortex lattice then propagates into the interior, driven forward by the elasticity of the vortex lattice and is slowed down by pinning and viscous resistance. The build up of the vortex lattice with decreasing temperature yields an increasing effective skin depth. However, a proper description of the observed enhancement of the skin depth calls for improved theory to account for the magnetic field arrangement used in ESR spectrometry (large static magnetic field, perpendicular mw perturbation, paralell rf magnetic field modulation).

IV. CONLCLUSION

In conlcusion, we observed and studied Conduction Electron Spin Resonance in the normal and superconducting state of CaC_6. The intercalation of graphite with calcium yields a more 2D crystal structure. However, electronically CESR characterizes CaC_6 as a 3D metal thus suggesting that Ca provides appreciable bonding between the graphene sheets along the c-axis. The temperature independent behavior of the spin lifetime, T_1, and the asymmetry parameter, A/B, provide evidence that the scattering processes of conduction electrons are dominated by impurity scattering and supports the description of superconductivity in the dirty limit. Nonlinear microwave absorption measurements in the superconducting state supports the description of CaC_6 as an anisotropic BCS superconductor. CESR data in the superconducting state indicate the vortex-enhancement of the effective skin depth below T_c, though the quantitative data analysis in the superconducting state requires the extension of theory to the magnetic field arrangement used in ESR spectroscopy. The study of the spin dynamics in the superconducting state of CaC_6 and the observation of the vortex enhanced increase of the skin depth calls for theoretical works to provide a comprehensive description of the observed phenomena.

ACKNOWLEDGEMENT

Part of this work was supported by German Research Foundation (DFG 436 UNG 17/4/05). F. M. greatfully acknowledges the fellowship of the Alexander von Humboldt Foundation.

[1] J. I. Kaplan, Phys. Lett., **19**, 266 (1965).
[2] P. G. deGennes, Solid State Comm., **4**, 95 (1966).
[3] K. Yosida, Phys. Rev., **110**, 769 (1958).
[4] Y. Yafet, Phys. Lett., **98A**, 287 (1983).
[5] D. C. Vier, S. Schultz, Phys. Lett., **98A**, 283 (1983).
[6] N. M. Nemes, J. E. Fischer, G. Baumgartner, L. Forro, T. Feher, G. Oszlanyi, F. Simon, A. Janossy, Phys. Rev. B, **61**, 7118 (2000).
[7] F. Simon, A. Janossy, T. Feher, F. Muranyi, S. Garaj, L. Forro, C. Petrovic, S. Budko, R. A. Ribeiro, P. C. Canfield, Phys. Rev. B, **72**, 012511 (2005).
[8] F. Simon, A. Janossy, F. Muranyi, T. Feher, H. Shimoda, Y. Iwasa, L. Forro, Phys. Rev. B, **61**, R3826 (2000).
[9] P. Lauginie, H. Estrade, J. Conard, D. Gurard, P. Lagrange, M. El Makrini, Physica, **99B**, 514 (1980).
[10] J. E. Weller, M. Ellerby, S. S. Saxena, R. P. Smith, N. T. Skipper, Nature Physics, **1**, 39 (2005).
[11] N. B. Hannay, T. H. Geballe, B. T. Matthias, K. Andres, P. Schmidt, D. MacNair, Phys. Rev. Lett., **14**, 225 (1965).
[12] R. A. Wachnik, L. A. Pendys, F. L. Vogel, P. Lagrange, Solid State Comm., **43**, 5 (1982).
[13] I. T. Belash, A. D. Bronnikov, O. V. Zharikov, A. V. Pal'nichenko, Synth. Met., **36**, 283 (1990).
[14] V. V. Avdeev, O. V. Zharikov, V. A. Nalimova, A. V. Pal'nichenko, K. N. Semenenko, Zh. Eksp. Teor. Fiz., **43**, 376 (1986).
[15] N. Bergeal, V. Dubost, Y. Noat, W. Sacks, D. Roditchev, N. Emery, C. Herold, J-F. Mareche, P. Lagrange, G. Loupias, Phys. Rev. Lett., **97**, 077003 (2006).
[16] G. Lamura, M. Aurino, G. Cifariello, E. Di Gennaro, A. Andreone, N. Emery, C. Hrold, J.-F. March, P. Lagrange, Phys. Rev. Lett., **96**, 107008 (2006).
[17] E. Jobiliong, H. D. Zhou, J. A. Janik, Y. -J. Jo, L. Balicas, J. S. Brooks, C. R. Wiebe, Phys. Rev. B, **76**, 052511 (2007).
[18] N. Emery, C. Hrold, P. Lagrange, J. Solid State Chem., **178**, 2947 (2005).
[19] M. S. Dresselhaus, G. Dresselhaus, Adv. in Phys., **51**, 1 (2002).
[20] F. J. Dyson, Phys. Rev., **98**, 349 (1955).
[21] G. Feher, A. F. Kip, Phys. Rev., **98**, 337 (1955).
[22] Y. Yafet, Solid State Physics, **14**, 1 (1963).
[23] A. Jnossy, R. Chicault, Physica C (Amsterdam), **192**, 399 (1992).
[24] K. W. Blazey, K. A. Muller, J. G. Bednorz, W. Berlinger, G. Amoretti, E. Buluggiu, A. Vera, F. C. Matacotta, Phys. Rev. B, **36**, 7241 (1987).
[25] M. K. Bhide, R. M. Kadam, M. D. Sastry, A. Singh, S. Sen, D. K. Aswal, S. K. Gupta, V. C. Sahni, Supercond. Sci. Tech., **14**, 572 (2001).
[26] G. Wagoner, Phys. Rev., **118**, 647 (1960).
[27] R. J. Elliott, Phys. Rev., **96**, 266 (1954).
[28] F. Beuneu, P. Monod, Phys. Rev. B, **18**, 2422 (1978).
[29] A. Gauzzi, S. Takashima, N. Takeshita, C. Terakura, H. Takagi, N. Emery, C. Herold, P. Lagrange, G. Loupias, Phys. Rev. Lett., **98**, 067002 (2007).
[30] J. S. Kim, L. Boeri, R. K. Kremer, F. S. Razavi, Phys. Rev. B, **74**, 214513 (2006).
[31] F. Murnyi, F. Simon, A. Jnossy, *unpublished results.*
[32] F. Simon, A. Janossy, T. Feher, F. Muranyi, S. Garaj, L. Forro, C. Petrovic, S. L. Bud'ko, G. Lapertot, V. G. Kogan, P. C. Canfield, Phys. Rev. Lett., **87**, 047002 (2001).
[33] Y. Kseoglu, B. Aktas, F. Yildiz, D. K. Kim, M. Toprak,

M. Muhammed, Physica C, **390**, 197 (2003).
[34] *Static magnetization measurements above H_{c2} also did not reveal traces of paramagnetic impurities.*
[35] D. H. Wu, S. Sridhar, Phys. Rev. Lett., **65**, 2074 (1990).
[36] E. H. Brandt, Phys. Rev. Lett., **67**, 2219 (1991).
[37] M. W. Coffey, J. R. Clem, Phys. Rev. B, **48**, 342 (1993).